Science Bulletin 63 (2018) 1470–1478

Contents lists available at ScienceDirect

Science Bulletin

journal homepage: www.elsevier.com/locate/scib

Science Bulletin
www.scibull.com

Article

Optimal photonic indistinguishability tests in multimode networks

Niko Viggianiello [a], Fulvio Flamini [a], Marco Bentivegna [a], Nicolò Spagnolo [a], Andrea Crespi [b,c], Daniel J. Brod [d,e], Ernesto F. Galvão [e], Roberto Osellame [b,c], Fabio Sciarrino [a,*]

[a] Dipartimento di Fisica, Sapienza Università di Roma, Piazzale Aldo Moro 5, I-00185 Roma, Italy
[b] Istituto di Fotonica e Nanotecnologie, Consiglio Nazionale delle Ricerche (IFN-CNR), Piazza Leonardo da Vinci, 32, I-20133 Milano, Italy
[c] Dipartimento di Fisica, Politecnico di Milano, Piazza Leonardo da Vinci, 32, I-20133 Milano, Italy
[d] Perimeter Institute for Theoretical Physics, 31 Caroline Street North, Waterloo, ON N2L 2Y5, Canada
[e] Instituto de Física, Universidade Federal Fluminense, Av. Gal. Milton Tavares de Souza s/n, Niterói, RJ 24210-340, Brazil

ARTICLE INFO

Article history:
Received 31 July 2018
Received in revised form 17 September 2018
Accepted 8 October 2018
Available online 25 October 2018

Keywords:
Particle indistinguishability
Quantum statistics
Optical quantum computation
Quantum simulation
Sylvester interferometers
Bayesian tests
Multiphoton interference experiments

ABSTRACT

Particle indistinguishability is at the heart of quantum statistics that regulates fundamental phenomena such as the electronic band structure of solids, Bose-Einstein condensation and superconductivity. Moreover, it is necessary in practical applications such as linear optical quantum computation and simulation, in particular for Boson Sampling devices. It is thus crucial to develop tools to certify genuine multiphoton interference between multiple sources. Our approach employs the total variation distance to find those transformations that minimize the error probability in discriminating the behaviors of distinguishable and indistinguishable photons. In particular, we show that so-called Sylvester interferometers are near-optimal for this task. By using Bayesian tests and inference, we numerically show that Sylvester transformations largely outperform most Haar-random unitaries in terms of sample size required. Furthermore, we experimentally demonstrate the efficacy of the transformation using an efficient 3D integrated circuits in the single- and multiple-source cases. We then discuss the extension of this approach to a larger number of photons and modes. These results open the way to the application of Sylvester interferometers for optimal assessment of multiphoton interference experiments.

1. Introduction

The observation that fundamental particles may be intrinsically indistinguishable is a counter-intuitive feature of quantum mechanics. As a consequence, their collective behaviour is governed by quantum statistics, and results in phenomena relevant in different contexts. For instance, many-body bosonic interference is at the very heart of quantum photonic computation [1–3]. In this context, Boson Sampling devices harness multiphoton interference effects to provide evidence of a superior quantum computational power with current state-of-the-art technology [3–15]. The task of certifying genuine many-boson interference is thus expected to find numerous applications in photonic quantum information, for validating the functioning of Boson Sampling experiments [8–11,16–28] and, more generally, as a diagnostic tool for quantum optical devices [29,30]. A well-known approach to experimentally test the degree of indistinguishability between photons involves the use of the Hong-Ou-Mandel effect [31], for which various generalizations have been proposed to account for multiple photon sources [32–38]. Given multiple photon sources, characterization of indistinguishability between the generated photons by using only pairwise Hong-Ou-Mandel experiments in a 50/50 beamsplitter presents some relevant limitations. When more than two photons are generated, pairwise mutual indistinguishability is not sufficient to fully characterize the landscape of multiphoton interference [37]. Furthermore, in the multiple-input scenario such as in scattershot Boson Sampling experiments [12,39,40], when several sources are connected in parallel and only a subset generates a single photon at each experimental run, separately measuring all pairwise two-photon indistinguishabilities does not represent an optimal solution. A natural problem that arises is then to determine which interferometers allow for an optimal assessment of the indistinguishability of multiphoton states, when only a single device is employed for the full set of input states (see Fig. 1).

In this work, we introduce a new approach for the task of discriminating distinguishable and indistinguishable photon behaviour in multimode photonic networks, and perform an experimental demonstration with two-photon inputs in laser-written integrated devices with an optimal interferometric design. Our

* Corresponding author.
E-mail address: fabio.sciarrino@uniroma1.it (F. Sciarrino).

https://doi.org/10.1016/j.scib.2018.10.009
2095-9273/

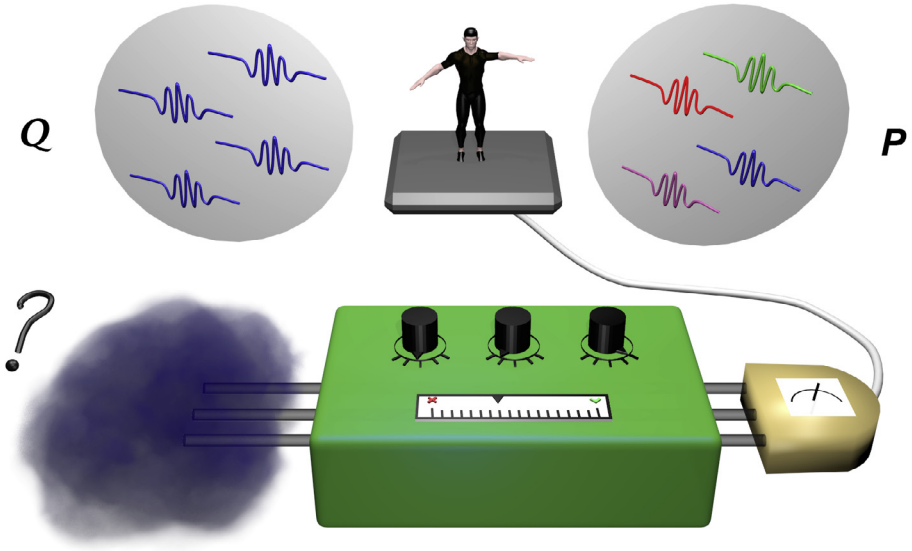

Fig. 1. (Color online) Searching for the optimal indistinguishability test. An unknown multiphoton state is injected into a multimode interferometer, designed to discriminate between the two hypotheses: either all photons are indistinguishable (Q) or all photons are distinguishable (P). The internal parameters can then be tuned until the most efficient test is found, for which the distributions corresponding to the two hypotheses P and Q are as different as possible, as measured by the total variation distance of the output distributions.

approach consists in identifying linear-optical interferometers for which the experimental output is as different as possible for the two distinguishability cases, according to a suitable figure of merit. Such interferometers will be optimal for indistinguishability tests, in the sense of requiring the least number of events for a given level of confidence in the discrimination problem. To assess the optimality of an interferometer we maximize the total variation distance (TVD) between the output probability distributions corresponding to indistinguishable and distinguishable photons, showing that in certain cases the optimal solution is provided by so-called Sylvester interferometers. More specifically, we prove optimality for variable-input 2-photon experiments in 4-mode interferometers, and provide numerical evidence of optimality for variable-input 2-photon experiments in 8-mode interferometers. We experimentally test our analysis by implementing two Sylvester interferometers with 4 and 8 modes, by adopting a 3-dimensional architecture enabled by the femtosecond laser micromachining technique. We then consider a setup in which probabilistic single-photon sources are coupled to different sets of input ports of an interferometer. Specifically, we perform a scattershot Boson Sampling experiment in the 4-mode Sylvester device by connecting all input modes with an heralded single-photon source, and verify the capability of the approach to validate the collected data by using a small number of events. Finally, we discuss the extension of this approach to systems with a larger number of photons and modes.

2. Optimal indistinguishability tests

In this section, we recall what the TVD is, and how it can be applied to our problem of estimating photon indistinguishability. Later on, in Sections 4 and 5, we provide numerical analyses based on Bayesian tests and Bayesian inference that showcase how a larger TVD results in more efficient distinguishability tests. In general, a linear interferometer is a device that implements a linear map between input and output creation operators, namely: $a^\dagger_{\mathrm{in}_k} \to \sum_j U_{j,k}\, a^\dagger_{\mathrm{out}_j}$. A m-mode interferometer is then completely specified by its corresponding $m \times m$ unitary matrix U, which can be decomposed into two-mode beam splitters and single-mode phase shifters [41]. The evolution of a n-photon state is ruled by the unitary transformation and by the degree of indistinguishability of the input particles. Let $P = \{p_i\}$ ($Q = \{q_i\}$) denote the output probability distribution of an interference experiment when the input photons, all injected in different input modes and including collision events, are perfectly distinguishable (indistinguishable) and the occupation number is detected at each output port. The TVD for a fixed input state is then defined as

$$T(P,Q) = \frac{1}{2}\sum_i |p_i - q_i|, \tag{1}$$

while we define $\overline{T}(P,Q)$ as the average of $T(P,Q)$ over all possible sets of n single-photon input modes. The TVD corresponds to the highest possible difference in probabilities that P and Q can assign to the same event. It is also closely related to hypothesis testing, since $1 - T(P,Q)$ is a lower bound on the sum of probabilities of false positive and false negative results [42]. More practically, a larger value of $T(P,Q)$ means that a smaller set of experimental data is sufficient to discriminate between the hypotheses that one is sampling from P or Q up to a given level of confidence. Indeed, the TVD actually determines the rate of convergence of the best possible statistical test that can be applied on the data sample, and hence does not depend on the computational complexity of any specific hypothesis test. The capability of ascertaining if the input photons are indistinguishable by using the lowest possible amount of data is relevant in practice, allowing for a verification of the sources with minimal use of resources. Given a specific choice of U, we then propose to employ the TVD between the two distributions $\{p_i\}$ and $\{q_i\}$ to quantify the interferometer's effectiveness at discriminating photon distinguishability. By maximising the TVD, our approach aims at finding, for each scenario (n,m), the optimal unitary transformation U_{opt} which discriminates between P and Q with the lowest possible number of measurements.

We consider two scenarios depending on how the input photons enter the interferometer: (i) the input ports are fixed (see Fig. 2a) and (ii) the input combination is randomly chosen for each event (see Fig. 2b). This second situation is typical of more sophisticated experiments with multiple probabilistic sources, such as

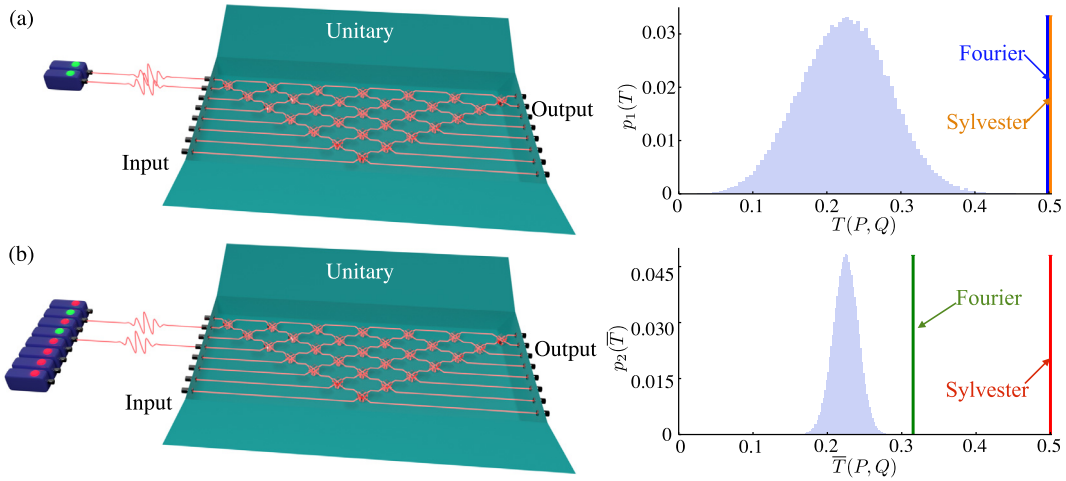

Fig. 2. (Color online) Optimal tests for fixed-input and scattershot configurations. (a) Left figure: fixed input configuration in the $n = 2,\ m = 8$ case, where two fixed input modes are injected with single photons. Right figure: estimate of the distribution $p_1(T)$ of the total variation distance $T(P,Q)$ for uniformly random unitaries in this scenario, obtained numerically by sampling over 10^5 unitaries. For specific choices of input modes, both Fourier (blue vertical bar) and Sylvester (orange vertical bar) interferometers are optimal. (b) Left figure: scattershot configuration in the $n = 2, m = 8$ case, where different sets of two input modes are picked at random. Right figure: estimate of the distribution $p_2(\overline{T})$ of the average total variation distance $\overline{T}(P,Q)$ for Haar-random unitaries in this scenario, obtained numerically by sampling over 10^5 unitaries. In this scattershot case the Sylvester transformation (red vertical bar) is optimal, while the Fourier is not.

scattershot Boson Sampling experiments [12,39]. Note that in the multiple-source scenario, measuring separately all pairwise Hong-Ou-Mandel interference patterns in a 50/50 beam-splitter is not optimal even in the case of two-photon inputs, since it requires performing a large set of independent experiments. In the next section we will search for a single interferometer able to characterize simultaneously the full set of sources. In case (ii), the relevant quantity to maximize is the average distance $\overline{T}(P,Q)$ over all sets of n single-photon input states, as described previously.

3. Optimal distinguishability tests in Sylvester and Fourier interferometers

To search for the optimal platform, in particular in the multiple-source scenario, a natural symmetry we can impose on the interferometer is that the output probability for single photons should be uniform for all input ports. Mathematically, this corresponds to a unitary matrix U with complex entries of modulus $1/d$, known as a Hadamard matrix. A specific subcase is provided by Sylvester transformations [43], described by $m = 2^p$-dimensional unitary matrices defined by the recursive rule:

$$S(2^p) = \begin{pmatrix} S\left(2^{p-1}\right) & S\left(2^{p-1}\right) \\ S\left(2^{p-1}\right) & -S\left(2^{p-1}\right) \end{pmatrix}, \tag{2}$$

with $S\left(2^0\right) = S(1) = (1)$ and p any positive integer. Another notable example of Hadamard matrix is the Fourier one:

$$\left(U_m^{\mathrm{F}}\right)_{l,q} = \frac{1}{\sqrt{m}} \mathrm{e}^{\mathrm{i}\frac{2\pi lq}{m}}, \tag{3}$$

which will be a second subject of our analysis. For two-photon experiments, we can apply 1 to check that the Sylvester transformation results, in the case of interferometers with $m = 4$ modes, in a $T_{\mathrm{S}} = 0.5$ independently of which pair of input modes is used, and thus on average (over different pairs of inputs) $\overline{T}_{\mathrm{S}} = 0.5$. As we show later, the Sylvester interferometer is optimal for all possible choices of two-photon input configurations. The Fourier interferometer results instead in a lower average $\overline{T}_{\mathrm{F}} = 0.333$, reaching the highest value $T_{\mathrm{F}} = 0.5$ only for cyclic inputs, i.e. n-photon Fock states in interferometers with n^p modes, where the occupied modes j_r^s are given by $j_r^s = s + (r-1)\,n^{p-1}$, with $r = 1,\ldots,n$ and $s = 1,\ldots,n^{p-1}$. For two-photon experiments in interferometers with $m = 8$ modes, among all known Hadamard matrices the Sylvester transformation is again the one with the largest average TVD $\overline{T}_{\mathrm{S}} = 0.5$ ($T_{\mathrm{S}} = 0.5$, and thus optimal, for all pairs of inputs). The Fourier interferometer reaches $T_{\mathrm{F}} = 0.5$ for cyclic inputs, while on average we obtain only $\overline{T}_{\mathrm{F}} = 0.3153$ due to inputs with lower TVD. The intuitive reason why Sylvester interferometers outperform Fourier ones is rooted in the higher symmetries of the former transformation, as apparent already in their definition in Eqs. (2) and (3). Specifically, the fact that the elements of Sylvester matrices are only ± 1 (real), while those of Fourier matrices can take 2^p different (complex) values, naturally makes the interference more fragile in the latter case with respect to the former. Here, with fragile we mean that fewer input-output combinations can fully enhance the effect of quantum interference, while changing just one input-output mode (l,q) can largely influence the dynamics. This feature is manifest both in the fixed-input scenario (where we only change the indexes associated to the output modes) as well as in the multiple-input scenario (where to evaluate the average TVD we also need to change the input combinations). Indeed, the two transformations become equivalent in the $m = 2$ case (and, hence, $n = 2$), leading to the well-known Hong-Ou-Mandel effect (HOM) in a beam splitter [31]. Intuitively, since the HOM is optimal to enhance the separation in TVD, the very structure of Sylvester matrices (which recursively copies the elements of a beam splitter with a symmetric pattern) explains why Sylvester matrices appear to be optimal for experiments with $n = 2$.

For variable input, two-photon experiments in the 4-mode Sylvester interferometer, optimality can be established with respect to any arbitrary transformation by using Reck et al.'s decomposition of general 4-mode unitaries [41] (see Section 1 of Supplementary Material for details). For two-photon experiments in $m = 8$ modes, a random sampling of 10^5 matrices uniformly drawn from the full set of transformations failed to find interferometers with higher TVD than the Sylvester. In Section 7 in the following and Section 1 of Supplementary Material we report the interferometers with highest TVD we found numerically for scenarios with larger number of photons and modes.

4. Experimental optimal distinguishability tests in Sylvester interferometers

To test our method, we experimentally demonstrate optimal distinguishability tests in the cases $n = 2$ and $m = (4, 8)$ using two custom-designed integrated photonic circuits fabricated on a glass substrate via the femtosecond laser writing technology [44–46]. A possible approach to the implementation of Fourier and Sylvester matrices on photonic platforms could exploit the decompositions of Refs. [41,47], which allow to implement arbitrary unitary operations through an in-plane cascade of beam-splitters and phase shifters but are sensitive against losses inside the device [48]. A more effective approach for the implementation of this class of interferometers is found by adopting an efficient, scalable and reliable three-dimensional interferometer design enabled by the interaction between non-first neighbor modes arranged in a suitable lattice [49] (Fig. 3). This architecture presents several advantages with respect to the above-mentioned conventional decomposition in beam splitters and phase shifters [41,47]. Indeed, this approach is efficient since it allows to significantly reduce the number of optical elements from $O(m^2)$ to $O(m \log m)$. There is also strong evidence that such architecture implements Fourier and Sylvester interferometer with the minimum number of optical elements. Furthermore, as shown in Section 2 of Supplementary Material, it is scalable to a larger number of modes. Finally, it is also reliable since the depth of the circuit is small $[O(\log\ m)]$ and the layout is symmetric with respect to the input modes, thus being intrinsically more robust against internal losses than the decomposition of Ref. [41]. These features permit to achieve higher fidelities in the implemented devices [48].

To probe the device for the reconstruction of its internal operation, we injected the interferometers with one- and two-photon states produced via a spontaneous parametric downconversion process [50]. The tomographic reconstruction of the processes exploits a priori knowledge of the internal structure, minimizing a suitable χ^2 function with respect to the unknown internal phases and transmissivities [19]. In Section 2 of Supplementary Material we provide more details about the design and the tomographic reconstruction. All tests have been carried out also on Fourier interferometers of equivalent dimensions ($m = 4, 8$), to provide a comparison between the two performances and highlight the advantages of the new approach. For more details on the implementation of the Fourier transforms refer to Ref. [19].

The TVD between distributions obtained from distinguishable and indistinguishable photons has been estimated experimentally for two-photon experiments in 4-mode and 8-mode Sylvester and Fourier interferometers. The two conditions are reached by properly introducing a relative temporal difference between the two photons using delay lines (see Section 3 of Supplementary Material). As previously discussed, a distinctive feature of Sylvester interferometers is that the TVD has the same value for two-photon experiments using any pair of input ports. This value is never outperformed by Fourier interferometers, being matched only for cyclic inputs.

In the case of the 4-mode Sylvester and Fourier interferometers, all $\frac{4!}{2!2!} = 6$ possible pairs of different input ports have been injected, thus considering all input states where photons enter from different ports. We measured for each pair all the collision-free output distributions (that is, events with at most one photon per output port), showing good agreement with the expected distribution. Additionally, we included in the distribution an extra bin accounting for the overall probability of collision events (see Fig. 4a). The adoption of this extra bin prevents the appearance of pathological unitaries in our numerical search, with high values of TVD for the collision-free subspace but unacceptably small probability of collision-free events, which strongly reduce the amount of detected signal (see Section 1 of Supplementary Material for more details). We then define the collision probability q_{coll} (p_{coll}) as the total probability of all events with more than one photon in one (or more) output ports. For distinguishable photons, this collision probability p_{coll} can be calculated using the measured probabilities for single-photon experiments. For indistinguishable photons, the additional information provided by the measured two-photon Hong-Ou-Mandel visibilities, together with the single-photon data, allows for an estimate of the collision probability q_{coll}. Adjusting the distinguishability of the input photons we could then estimate the TVD according to Eq. (1). The experimental results are reported in Fig. 4b. In the fixed input case, the Sylvester interferometer (for all inputs) and the Fourier one (only for cyclic inputs) reaches similar values within the range $0.435 \leqslant T^{(4)} \leqslant 0.461$. When averaging

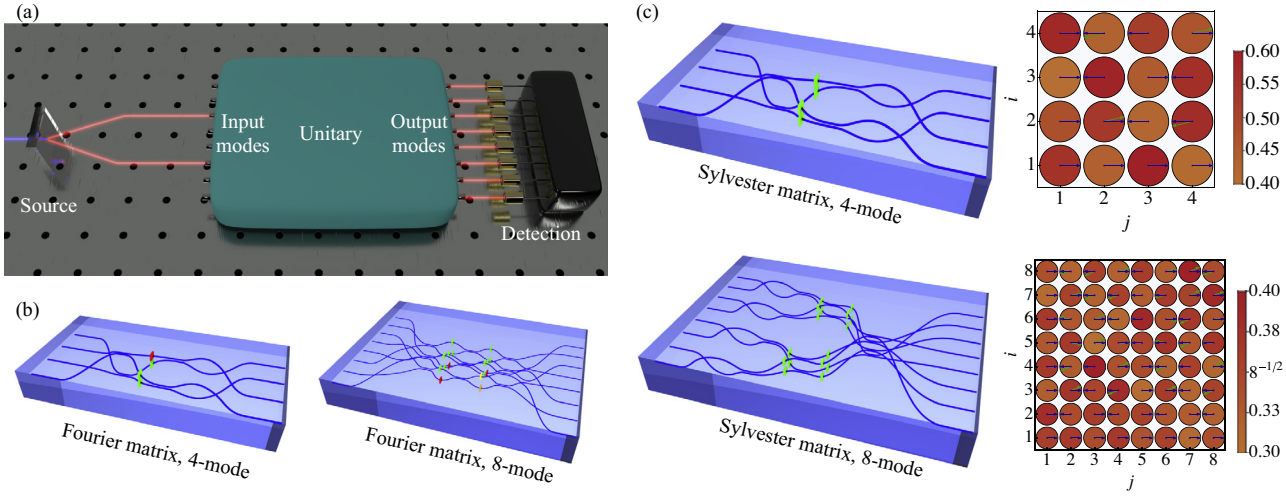

Fig. 3. (Color online) Scheme of the experimental approach for the optimal test. (a) A photon source based on parametric down-conversion produces pairs of photons that can be injected in any possible input combination of a unitary transformation, with photodetection at the output. (b) Internal structure for the 4- and 8-mode laser-written Fourier interferometers. (c) Internal structures for the 4-mode and 8-mode implemented Sylvester interferometers, and corresponding representation of the tomographically reconstructed matrices: disk color indicates the modulus of each matrix element, with an arrow representing its phase (green: reconstructed unitary, blue: theoretical matrix). In the circuital structures of panels (b) and (c), colored boxes correspond to phase shifters. Green boxes: $\phi = 0$. Red boxes: $\phi = \pi/2$. Orange boxes: $\phi = 3\pi/4$. Yellow boxes: $\phi = \pi/4$.

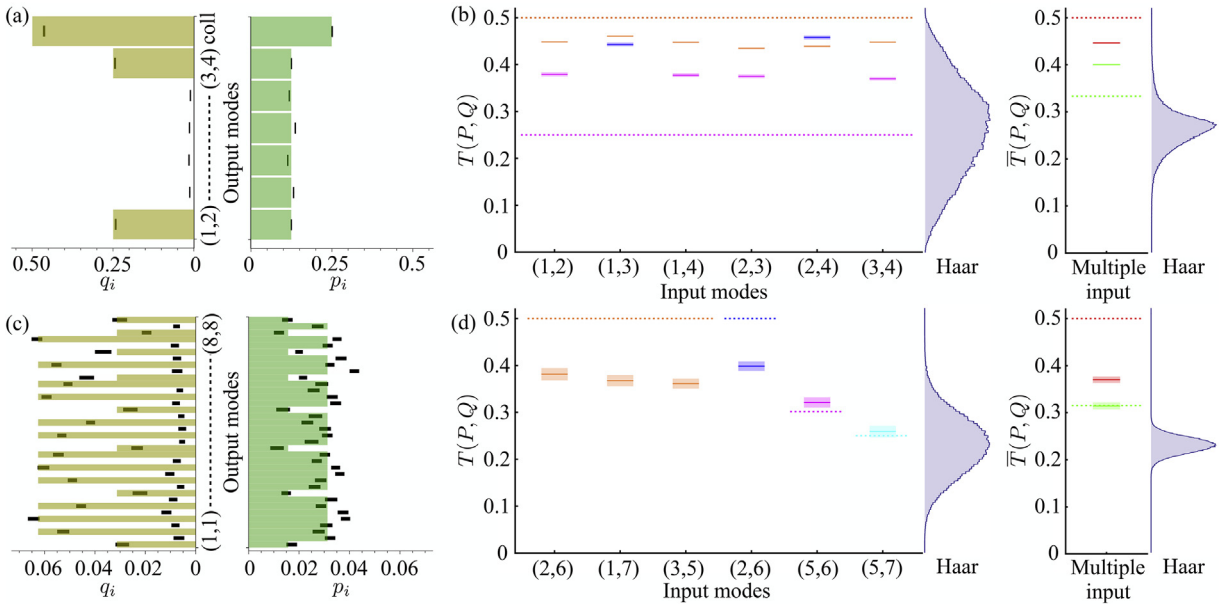

Fig. 4. (Color online) Experimental data from Sylvester interferometers and comparison with Fourier ones. Two-photon experimental data from 4-mode and 8-mode Sylvester interferometer. (a), (c) Output probability distributions measured as a function of output mode combinations (i,j) for (a) input (1,2) of the 4-mode Sylvester interferometer and (c) input (1,5) of the 8-mode interferometer. Each plot compares the distributions obtained from indistinguishable (yellow) and distinguishable (green) input photons. The additional bar *coll.* in (a) is the collision probability q_{coll} (p_{coll}) for indistinguishable (distinguishable) particles, taking into account all collision events. Colored bars show the ideal probability distribution, while error bars in the distributions are due to the Poissonian statistics of the measured photon counts. (b), (d) Total variation distances between the measured output distributions for indistinguishable and distinguishable photons in the 4-mode (b) and 8-mode (d) interferometers, plotted for each fixed input (left) and for the multiple input configuration (right). On each plot, the distributions of $T(P,Q)$ and $\overline{T}(P,Q)$ for Haar-random transformations (obtained by sampling 10^5 unitaries) are shown. Legend - Rectangles: 1σ regions for the experimental data, obtained from the Poissonian statistics of the measured photon count. Dashed lines: theoretical predictions for ideal interferometers. For $m = 4$, the expected values are obtained by using the extra collision bin. Red: Sylvester matrix, multiple input. Green: Fourier matrix, multiple input. Orange: Sylvester, fixed input. Blue: Fourier, fixed cyclic inputs. Purple, Cyan: Fourier, fixed non-cyclic inputs.

over all inputs, the 4-mode Sylvester interferometer results in $\overline{T}_{\text{S}}^{(4)} = 0.4465 \pm 0.0006$, thus clearly outperforming the Fourier interferometer that yields $\overline{T}_{\text{F}}^{(4)} = 0.4003 \pm 0.0016$. As previously discussed, higher values of the TVD correspond to lower number of measurements necessary to discriminate between the two hypotheses (see also Section 5 below). In the case of the 8-mode interferometers, all two-photon output events were measured, including those with collisions (see Fig. 4c), showing good agreement with the expected distribution. We probed the interferometers with three different pairs of input ports, corresponding to the three classes of input pairs that, for the Fourier interferometer, result in different TVDs. Given the quality of the reconstructed transformations, we expect that all other input combinations will lead to similar values of the TVDs. Again, the TVD for the Fourier interferometer reaches the same value of the Sylvester only for cyclic input pairs. The measured average values were $\overline{T}_{\text{F}}^{(8)} = 0.314 \pm 0.007$ and $\overline{T}_{\text{S}}^{(8)} = 0.370 \pm 0.007$, where the average $\overline{T}_{\text{F}}^{(8)}$ was estimated by weighting the three representative input states by the multiplicity of the corresponding classes with different TVDs (Fig. 4d). Deviation of the experimentally measured values from the expected ones depend on manufacturing errors and partial photon indistinguishability. For Sylvester interferometers, both such experimental errors tend to reduce the values of the TVD. Curiously, for Fourier interferometers the measured $\overline{T}_{\text{F}}^{(4)}$ and $\overline{T}_{\text{F}}^{(8)}$ are higher than what was expected theoretically. Indeed, as we show in Section 4 of Supplementary Material, a particular feature of the Fourier interferometric design is that manufacturing errors can result in interferometers which are closer to the Sylvester one, thus increasing the TVD. This feature is obtained when fabrication errors induce a value of the internal phases closer to the one of a Sylvester interferometer. We performed the same analysis with 10^5 unitaries, randomly sampled according to the Haar measure, showing that the mean values of their TVDs are lower than both Fourier and Hadamard (see Fig. 4b,d). Our results are compatible with the theoretical prediction that the adoption of Sylvester interferometers maximizes the difference between the behavior of distinguishable and indistinguishable photons in all scenarios (fixed and multiple input), outperforming, in particular, Fourier interferometers in the multiple input configuration.

5. Bayesian hypothesis test

At the core of our approach lies the idea that a larger TVD allows us to discriminate more readily the two hypotheses (distinguishable or indistinguishable photons). To illustrate this feature, in Fig. 5a–d we show the results of a Bayesian analysis with data samples numerically generated from the measured distributions, compared with those expected from ideal transformations (see Ref. [17], Sections 5, 6 of Supplementary Material for more details on the Bayesian validation test). For a given sample size, we use a likelihood ratio test [17] to update a prior which initially assigns equal probabilities to the two hypotheses P and Q, thus assuming no a priori knowledge. To verify the optimality of Sylvester interferometers in terms of minimum sample size, the results obtained are compared with a sample of 10^4 Haar-random unitaries. The figure of merit is the confidence probability P_{conf} that a data sample is assigned to the corresponding correct hypothesis. While experimental imperfections might lead to a subset of Haar random unitaries with higher P_{conf} than experimental data (for $N_{\text{ev}} > 10$), we show in Fig. 5e–f that ideal Sylvester interferometers always outperform Haar random transformation. Notwithstanding, the gain obtained by using Sylvester interferometers is observed for low values of the number of collected events, for both experimental data and the ideal case.

Note that the dispersion of P_{conf} for Haar-random unitaries in the fixed-input case is larger than in the multiple-input configuration. To verify how strict the validation test is, we need to consider

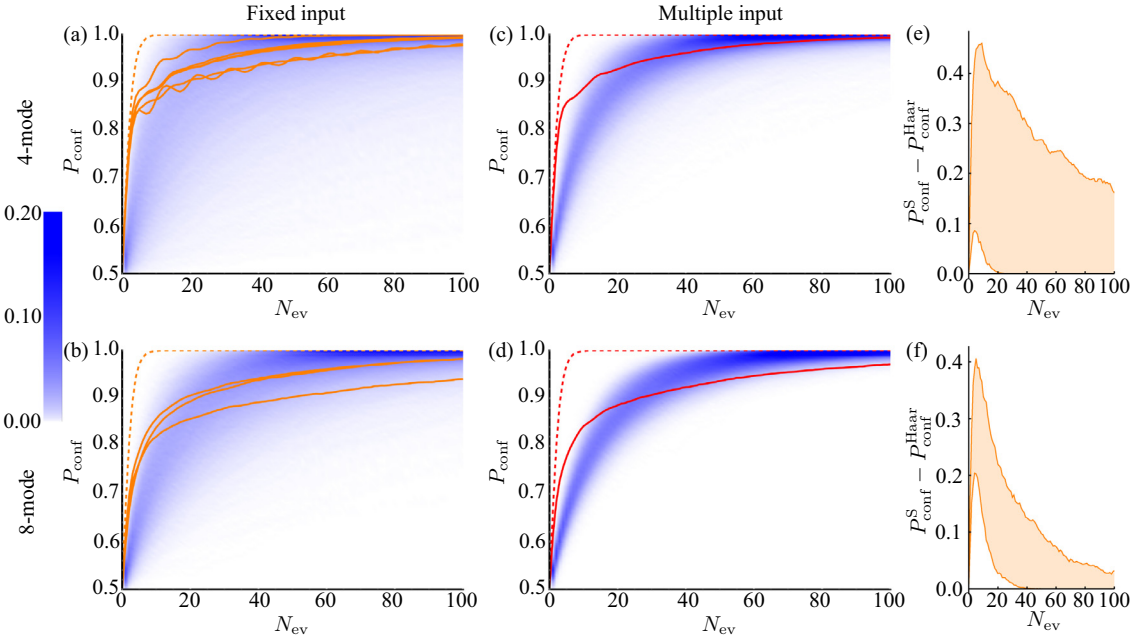

Fig. 5. (Color online) Bayesian simulation of hypothesis testing. Probability $P_{\rm conf}$ of correctly identifying the type of data sample (distinguishable or indistinguishable photons) in a Bayesian test, as a function of sample size (number of events), for the Sylvester interferometer. (a) 4-mode interferometer, fixed input states. (b) 8-mode interferometer, fixed input states. (c) 4-mode interferometer, multiple input configuration. (d) 8-mode interferometer, multiple input configuration. For the 8-mode devices, inputs used were (2,6), (1,7), (3,5). Dashed curves: theoretical predictions for an ideal Sylvester interferometer. Solid curves: average of 10^4 distinct samples generated numerically from the experimentally measured distributions. Red curves: Sylvester matrix, multiple input configuration. Orange curves: Sylvester matrix, different input states. Blue regions: contour plots obtained from a numerical simulation over 10^4 Haar-random matrices. Simulated data for the Haar-random case include partial photon indistinguishability $x\prime = 0.95$ equal to the experimental data, characterized by performing Hong-Ou-Mandel interference in a 50/50 beam-splitter. (e), (f) Increase in the confidence probability $P^{S}_{\rm conf} - P^{\rm Haar}_{\rm conf}$ obtained by using an ideal Sylvester interferometer with respect to Haar random transformations as a function of the number of collected events $N_{\rm ev}$. Shaded regions show the full interval for $P^{S}_{\rm conf} - P^{\rm Haar}_{\rm conf}$ obtained by sampling 10^4 Haar random unitaries for $n = 2$ and $m = 4$ (e), $m = 8$ (f).

the effect of partial photon indistinguishability. This can be done by considering that the output distribution $\{h_i(x)\}$ in the general two-photon case can be written as a convex combination $h_i(x) = xq_i + (1-x)p_i$, where $x \in [0;1]$ is a real parameter quantifying the amount of photon indistinguishability. Numerical simulations performed on the Bayesian test show that, by including this effect, photons pass the test if $x > 0.788$ for the 4-mode interferometer and $x > 0.685$ for the 8-mode case (see Section 7 of Supplementary Material). In the two-photon case, other sources of noise such as multiple pair emission in parametric down-conversion sources or spectral correlations [51] can be operationally included in the parameter x resulting in a lower effective indistinguishability between the photons. All measurements reported up to here were performed with a single two-photon source, for which the value of x was $x\prime = 0.95$, characterized by performing Hong-Ou-Mandel experiments in a 50/50 beam-splitter. This will change in the next section, where we consider an experiment with multiple sources.

6. Experimental scattershot Boson Sampling

Scattershot Boson Sampling has been shown [12] to enable scalable Boson Sampling experiments using probabilistic single-photon sources, at the cost of using a larger number of single-photon sources at the input. To show that our approach works well for this multiple-input configuration, we have performed a scattershot Boson Sampling experiment by connecting each input mode of our 4-mode Sylvester interferometer to an independent heralded parametric down-conversion source (see Fig. 6a). This single setup simultaneously samples all 6 different two-photon input states. We have collected data both for the indistinguishable and distinguishable photon cases, obtained by appropriately adjusting the relative time delay between the input paths. We will now move a step forward with respect to the previous binary Bayesian test (that is, evaluating which is the most likely hypothesis between Q and P). Specifically, we consider a different scenario where the aim is to assess the output data by estimating the value of the mutual indistinguishability of the PDC sources in the scattershot experiment. As we discussed, the output distribution in the general two-photon case is described by $\{h_i(x)\}$ with $x \in [0;1]$, and the set of hypotheses to be tested is now provided by a convex combination of indistinguishable Q (distinguishable P) photons $H(x) = xQ + (1-x)P$. We have then applied Bayesian inference [52,53] to the measured experimental data to estimate the value of x, starting from a uniform prior $\mathscr{P}(x)$ and subsequently updating the distribution according to the Bayes rule after the observation of a given data sample (see Section 8 of Supplementary Material for more details on this approach).

Fig. 6b,c show the results of the Bayesian inference performed by using the measured − experimental scattershot data samples (in this case, no extra bin for collision events has been included). The final estimated value $\tilde{x}_{\rm est}$ of the indistinguishability parameter x, obtained by using the complete set of experimental data, is $\tilde{x}_{\rm est}$. Here, we assumed that all (identical) photon sources present the same value of x, and thus this estimated value corresponds to an average value. Such value is compatible with the one obtained from a characterization with Hong-Ou-Mandel interference in a 50/50 beam-splitter $x_{\rm HOM} = 0.79 \pm 0.06$, and with the estimated interval obtained with an alternative method based on binary likelihood ratio tests $x_{\rm LR} \in [0.734; 0.742]$ (see Section 8 of Supplementary Material). Note that this value is different from the one corresponding to the single source measurements discussed in previous sections, where $x_2 = 0.95$. Indeed, in this case all two-photon combinations are obtained with photons generated from different sources, which results in lower values of indistinguishability.

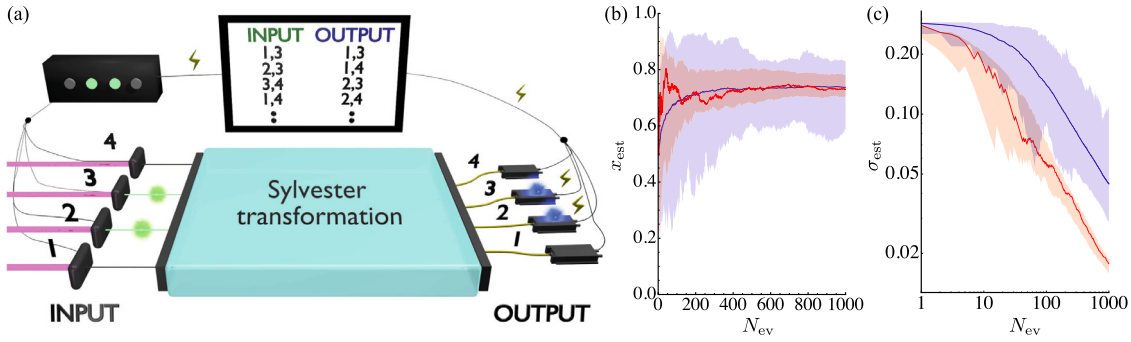

Fig. 6. (Color online) Bayesian inference on experimental scattershot Boson Sampling. Inference of the photon indistinguishability x as a function of sample size (number of events) from two-photon scattershot Boson Sampling experimental data in a 4-mode Sylvester chip. (a) Experimental scheme of the scattershot apparatus. We use four different PDC sources to probabilistically inject all input states, where each source is connected to exactly one trigger detector and one input mode. The two-photon output states are retrieved from heralded 4-fold coincidences (two trigger detectors and two output detectors). (b) Evolution of the estimated value x_{est} as a function of the number of events and (c) error σ_{est} inferred on the estimated value x_{est} from the Bayesian posterior distribution with the 4-mode interferometer (experimental data) as a function of the number of events N_{ev}, compared with Haar-random matrices (numerical simulations). Red solid line: estimation process using a single data sequence for the Sylvester interferometer. Red shaded region: interval spanned by $M = 100$ different data sequences generated by random permutations of the experimentally measured data. Blue solid line: average value obtained by numerically sampled $M = 100$ Haar-random unitaries. Blue shaded region: interval obtained by numerically sampling $M = 100$ Haar-random unitaries. The value of x adopted for the Haar-random numerical simulations (blue shaded region) is equal to the final value $\bar{x}_{est}$ estimated from the full set of experimental data.

The performance obtained with the experimental data on Sylvester interferometer are then compared with the one achievable with Haar random transformations, showing its capability to acquire information on photon input at a faster rate than any other interferometer. Indeed, the value of the estimation error σ_{est} is lower with respect to the Haar ensemble (for the same number of measured events N_{ev}). This confirms that Sylvester interferometers represent a promising platform for the assessment of photon indistinguishability of multiple sources. Moreover, Bayesian inference is shown to be an effective tool in estimating the degree of distinguishability between different sources, which can turn particularly useful where separate Hong-Ou-Mandel tests are unfeasible or not applicable.

7. Optimal interferometers for larger number of photons

Our approach uses the TVD to identify optimal interferometers for the task of discriminating photon distinguishability. In Section 3 we showed Sylvester interferometers are optimal for variable-input, 2-photon experiments in 4-mode interferometers, and provided numerical evidence that they are optimal also for 2-photon experiments in 8-mode interferometers. We will now show, however, that for larger number of photons and modes the TVD-maximizing interferometers may even be non-Hadamard. In this section we report some of our numerical findings in the search for TVD-maximizing interferometers for scenarios with more than two input photons. We also report on simulations of parameter estimation in the multi-photon regime.

In the multiple-input case, we have seen that Sylvester interferometers seem to be optimal for the case of two-photon experiments. For a larger number of photons, however, other interferometers may result in higher TVD than the Sylvester and Fourier transformations. The key here is to search among non-Hadamard interferometers as well. For N_{ev}, the best design we found corresponds to the unitary matrix

$$U_4 = \frac{1}{2}\begin{pmatrix} 1 & 1 & \sqrt{2} & 0 \\ 1 & -1 & 0 & \sqrt{2} \\ 1 & 1 & -\sqrt{2} & 0 \\ 1 & -1 & 0 & -\sqrt{2} \end{pmatrix}, \tag{4}$$

with average $\overline{T}_{U_4} = 0.53125$, beating for example the Fourier and Sylvester interferometers, which result in $\overline{T} = 0.3125$.

Even in the fixed-input scenario, there exist non-Hadamard interferometers resulting in higher TVD than the Fourier transform. For example, for $n = 4$ consider the following 6-mode interferometer:

$$U_8 = \frac{1}{\sqrt{6}}\begin{pmatrix} 1 & \sqrt{3} & 1 & 0 & 1 & 0 \\ 1 & -\sqrt{3} & 1 & 0 & 1 & 0 \\ 1 & 0 & e^{\frac{2i\pi}{3}} & \sqrt{3} & e^{-\frac{2i\pi}{3}} & 0 \\ 1 & 0 & e^{\frac{2i\pi}{3}} & -\sqrt{3} & e^{-\frac{2i\pi}{3}} & 0 \\ 1 & 0 & e^{-\frac{2i\pi}{3}} & 0 & e^{\frac{2i\pi}{3}} & \sqrt{3} \\ 1 & 0 & e^{-\frac{2i\pi}{3}} & 0 & e^{\frac{2i\pi}{3}} & -\sqrt{3} \end{pmatrix}. \tag{5}$$

With 4 photons in input ports $1, 2, 3$, and 5, the TVD (including collisions) is $T_{U_8} = 19/24 \approx 0.792$, as compared to largest fixed-input TVD values $0.750, 0.344, 0.639$ for the Fourier transforms of 4, 5, and 6 modes, respectively. This shows that when $n > 2$ the TVD-maximizing interferometers may be non-Hadamard interferometers with more modes than input photons. In Section 1 of Supplementary Material we report the best interferometers we have found numerically for a number of different scenarios. An interesting remaining open problem consists in finding better interferometers for each scenario, if possible proving their optimality.

The Bayesian hypothesis test discussed in Section 5 can be directly applied in the multiphoton regime to discriminate between the two hypotheses Q (indistinguishable photons) and P (distinguishable ones). In Fig. 7a we show the results of a numerical simulation for the case ($n = 3$, $m = 8$, fixed input), using the best transformation we found, the matrix U_{11}, which consists of a 3-mode Fourier transform, with identity in the remaining modes. In Fig. 7b we simulate the case (U_{11}, multiple input), using an 8-mode Sylvester interferometer. In both cases, we observe that the adoption of a transformation with high TVD allows us to achieve a high confidence probability P_{conf} for a very limited number of measured events P_{conf}, clearly outperforming the success rate achieved with Haar-random matrices.

An interesting feature of the multiphoton scenario is that pairwise two-photon indistinguishability is not sufficient to fully characterize the landscape of multiparticle interference. Indeed, some additional parameters that cannot be detected by performing two-photon Hong-Ou-Mandel contribute to the output pattern [37]. For instance, in the three-photon case an additional phase φ has to be added to the three mutual indistinguishabilities φ. Instead, such parameters can be effectively characterized with

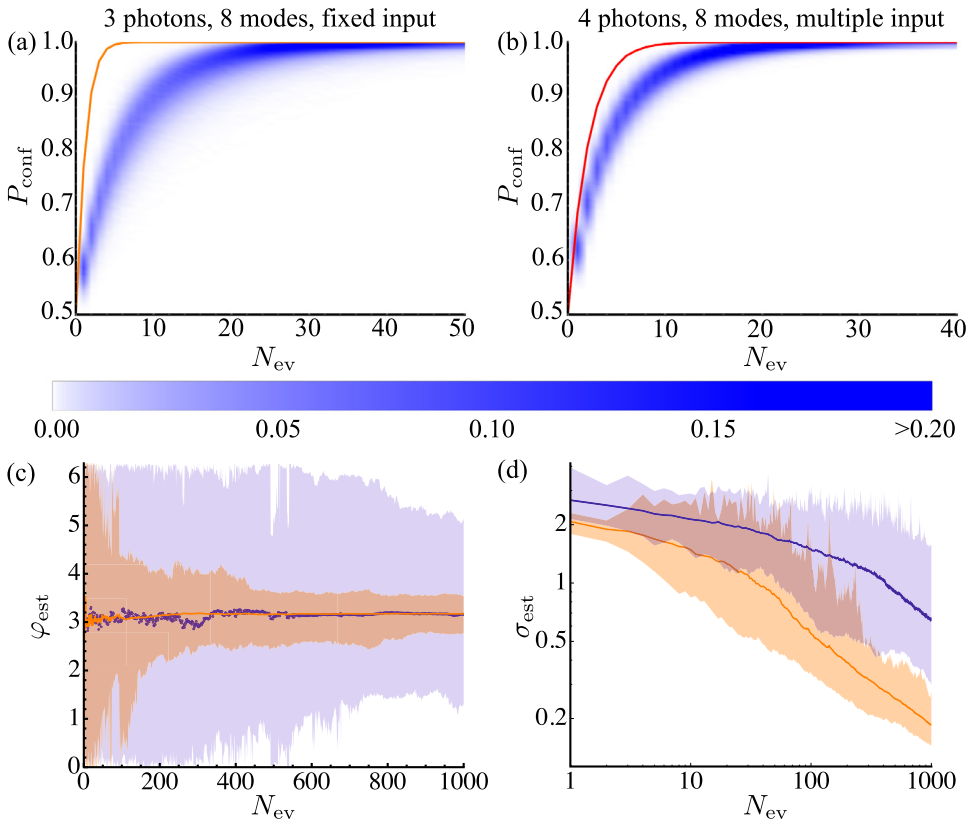

Fig. 7. (Color online) Numerical simulations of Bayesian hypothesis testing and Bayesian inference in the multiphoton scenario. (a), (b) Confidence probability of correctly identifying the type of data sample (distinguishable or indistinguishable photons) in a Bayesian test, as a function of sample size (number of events). (a) 3 photons in a 8-mode interferometer, fixed input configuration. (b) 4 photons in a 8-mode interferometer, multiple input configuration. Curves: optimal interferometer for the problem size ((a) matrix U_{11}, orange; (b) Sylvester interferometer, red). Blue regions: contour plots obtained from a numerical simulation over 10^4 Haar-random matrices. (c), (d) Inference of the three-photon phase φ in a $n = 3,\ m = 8$ fixed input scenario for mutual indistinguishabilities $x_{12} = x_{13} = x_{23} = 1/2$. Solid lines: average values obtained by numerically sampling $M = 100$ Haar-random unitaries (blue) and by numerically simulating 10^4 estimation processes with the optimal matrix U_{11} (orange). Shaded regions: intervals obtained by numerically sampling $M = 100$ Haar-random unitaries (blue) and by numerically simulating 10^4 estimation processes with the optimal matrix U_{11} (orange).

our method, by applying a continuous hypothesis testing similar to the one discussed in Section 5 for the scattershot experiment. In Fig. 7c,d we report a numerical simulation of an estimation of φ using 3-photon experiments in interferometer U_{11}, as well as in an ensemble of Haar-random interferometers (for comparison).

8. Discussion and conclusion

In summary, in this work we propose a method to search for optimal interferometer designs to ascertain photon indistinguishability in multiparticle interference experiments, showing that in certain scenarios Sylvester transformations offer an optimal solution for all input configurations in terms of the required sampled size. We then experimentally implement these interferometers by exploiting a recently introduced 3D-architecture enabled by femtosecond laser-writing technology. We verify the superior performance of Sylvester interferometers with a Bayesian hypothesis test which correctly identifies whether photons are distinguishable or not using very small data sets. Furthermore, we perform a complete scattershot Boson Sampling experiment with the implemented Sylvester device, showing the capability of identifying the collected data in this more complex multiple input configuration. Several perspectives can be envisaged starting from these results.

On the experimental side, Sylvester and other optimal interferometers suggest an immediate application in the assessment of scattershot Boson Sampling, that enables scalable experiments even with probabilistic single-photon sources. Furthermore, this class of transformations can represent a promising platform for near-future investigations on deterministic single photon sources [54–57], in order to fully characterize multiphoton interference [13–15,37], and as a diagnostic tool in reconfigurable photonic devices [11,58].

On the theoretical side, an outstanding open problem concerns the identification of optimal interferometer designs for scenarios comprising different interferometer sizes, number of photons, and for fixed or multiple inputs. Surprisingly, even for fixed inputs there exist non-trivial interferometers surpassing the performance of Fourier interferometers, as our example φ in Section 7 shows.

Conflict of interest

The authors declare that they have no conflict of interest.

Acknowledgments

This work was supported by ERC-Starting Grant 3D-QUEST (3D-Quantum Integrated Optical Simulation; Grant agreement No. 307783), H2020-FETPROACT-2014 Grant QUCHIP (Quantum Simulation on a Photonic Chip; Grant agreement No. 641039), Brazilian National Institute for Science and Technology of Quantum Information (INCT-IQ/CNPq) and in part by Perimeter Institute for Theoretical Physics.

Appendix A. Supplementary data

Supplementary data associated with this article can be found, in the online version, at https://doi.org/10.1016/j.scib.2018.10.009.

References

[1] Knill E, Laflamme R, Milburn GJ. A scheme for efficient quantum computation with linear optics. Nature 2001;409:46–52.
[2] Nielsen MA, Chuang IL. Quantum computation and quantum information. Cambridge University Press; 2010.
[3] Aaronson S, Arkhipov A. The computational complexity of linear optics. Proceedings of the 43rd annual ACM symposium on Theory of Computing. ACM Press; 2011. p. 333–42.
[4] Broome MA, Fedrizzi A, Rahimi-Keshari S, et al. Photonic boson sampling in a tunable circuit. Science 2013;339:794–8.
[5] Spring JB, Metcalf BJ, Humphreys PC, et al. Boson sampling on a photonic chip. Science 2013;339:798–801.
[6] Tillmann M, Dakic B, Heilmann R, et al. Experimental boson sampling. Nat Photonics 2013;7:540–4.
[7] Crespi A, Osellame R, Ramponi R, et al. Integrated multimode interferometers with arbitrary designs for photonic boson sampling. Nat Photonics 2013;7:545–9.
[8] Spagnolo N, Vitelli C, Sansoni L, et al. General rules for bosonic bunching in multimode interferometers. Phys Rev Lett 2013;111:130503.
[9] Carolan J, Meinecke JDA, Shadbolt PJ, et al. On the experimental verification of quantum complexity in linear optics. Nat Photonics 2014;8:621–6.
[10] Spagnolo N, Vitelli C, Bentivegna M, et al. Experimental validation of photonic boson sampling. Nat Photonics 2014;8:615–20.
[11] Carolan J, Harrold C, Sparrow C, et al. Universal linear optics. Science 2015;349:711–6.
[12] Bentivegna M, Spagnolo N, Vitelli C, et al. Experimental scattershot boson sampling. Sci Adv 2015;1:e1400255.
[13] Loredo JC, Broome MA, Hilaire P, et al. Boson sampling with single-photon fock states from a bright solid-state source. Phys Rev Lett 2017;118:130503.
[14] Wang H, He Y, Li YH, et al. High-efficiency multiphoton boson sampling. Nat Photonics 2017;11:361–5.
[15] He Y, Ding X, Su Z-E, et al. Time-Bin-encoded boson sampling with a single-photon device. Phys Rev Lett 2017;118:190501.
[16] Aaronson S, Arkhipov A. Boson sampling is far from uniform. Quan Inf Comput 2014;14:1383–423.
[17] Bentivegna M, Spagnolo N, Vitelli C, et al. Bayesian approach to boson sampling validation. Int J Quant Inf 2014;12:1560028.
[18] Tichy MC, Mayer K, Buchleitner A, et al. Stringent and efficient assessment of boson-sampling devices. Phys Rev Lett 2014;113:020502.
[19] Crespi A, Osellame R, Ramponi R, et al. Suppression law of quantum states in a 3D photonic fast fourier transform chip. Nat Commun 2016;7:10469.
[20] Liu K, Lund AP, Gu YJ, et al. A certification scheme for the boson sampler. J Opt Soc Am B 2016;33:1835–41.
[21] Walschaers M, Kuipers J, Urbina JD, et al. Statistical benchmark for boson sampling. New J Phys 2016;18:032001.
[22] Bentivegna M, Spagnolo N, Sciarrino F. Is my boson sampler working? New J Phys 2016;18:041001.
[23] Shchesnovich VS. Universality of generalized bunching and efficient assessment of boson sampling. Phys Rev Lett 2016;116:123601.
[24] Wang J, Bonneau D, Villa M, et al. Chip-to-chip quantum photonic interconnect by path-polarization interconversion. Optica 2016;3:407–13.
[25] Agresti I, Viggianiello N, Flamini F, et al. Pattern recognition techniques for boson sampling validation. arXiv:1712.06863, 2017.
[26] Giordani T, Flamini F, Pompili M, et al. Experimental statistical signature of many-body quantum interference. Nat Photonics 2018;12:173–8.
[27] Viggianiello N, Flamini F, Innocenti L, et al. Experimental generalized quantum suppression law in Sylvester interferometers. New J Phys 2018;20:033017.
[28] Dittel C, Dufour G, Walschaers M, et al. Totally destructive interference for permutation-symmetric many-particle states. Phys Rev A 2018;97:062116.
[29] Aolita L, Gogolin C, Kliesch M, et al. Reliable quantum certification of photonic state preparations. Nat Commun 2015;6:8498.
[30] Spring J B, Mennea P L, Metcalf B J, et al. Chip-based array of near-identical, pure, heralded single-photon sources. Optica 2017;4:90–6.
[31] Hong CK, Ou ZY, Mandel L. Measurement of subpicosecond time intervals between two photons by interference. Phys Rev Lett 1987;59:2044–6.
[32] Ou ZY, Mandel L. Violation of bell's inequality and classical probability in a two-photon correlation experiment. Phys Rev Lett 1988;61:50.
[33] Walborn SP, Oliveira AN, Padua S, et al. Multimode hong-ou-mandel interference. Phys Rev Lett 2003;90:143601.
[34] Sagioro MA, Olindo C, Monken CH, et al. Time control of two-photon interference. Phys Rev A 2004;69:053817.
[35] Spagnolo N, Vitelli C, Aparo L, et al. Three-photon bosonic coalescence in an integrated tritter. Nat Commun 2013;4:1606.
[36] Tillmann M, Tan S-H, Stoeckl SE, et al. Generalized multiphoton quantum interference. Phys Rev X 2015;5:041015.
[37] Menssen AJ, Jones AE, Metcalf BJ, et al. Distinguishability and many-particle interference. Phys Rev Lett 2017;118:153603.
[38] Agne S, Kauten T, Jin J, et al. Observation of genuine three-photon Interference. Phys Rev Lett 2017;118:153602.
[39] Lund AP, Laing A, Rahimi-Keshari S, et al. Boson sampling from a gaussian state. Phys Rev Lett 2014;113:100502.
[40] Latmiral L, Spagnolo N, Sciarrino F. Towards quantum supremacy with lossy scattershot boson sampling. New J Phys 2016;18:113008.
[41] Reck M, Zeilinger A, Bernstein HJ, et al. Experimental realization of any discrete unitary operator. Phys Rev Lett 1994;73:58–61.
[42] Lehmann EL, Romano JP. Testing statistical hypotheses. Springer Texts in Statistics, 2005.
[43] Crespi A. Suppression laws for multiparticle interference in sylvester interferometers. Phys Rev A 2015;91:013811.
[44] Osellame R, Taccheo S, Marangoni M, et al. Femtosecond writing of active optical waveguides with astigmatically shaped beams. J Opt Soc Am B 2003;20:1559–67.
[45] Della Valle G, Osellame R, Laporta P. Micromachining of photonic devices by femtosecond laser pulses. J Opt A 2009;11:013001.
[46] Marshall GD, Politi A, Matthews JCF, et al. Laser written waveguide photonic quantum circuits. Opt Express 2009;17:12546–54.
[47] Clements WR, Humphreys PC, Metcalf BJ, et al. Optimal design for universal multiport interferometers. Optica 2016;3:1460–5.
[48] Flamini F, Spagnolo N, Viggianiello N, et al. Benchmarking integrated linear-optical architectures for quantum information processing. Sci Rep 2017;7:15133.
[49] Barak R, Ben-Aryeh Y. Quantum fast fourier transform and quantum computation by linear optics. J Opt Soc Am B 2007;24:231–40.
[50] Burnham DC, Weinberg DL. Observation of simultaneity in parametric production of optical photon pairs. Phys Rev Lett 1970;25:84–7.
[51] Miková M, Fikerová H, Straka I, et al. Carrying qubits with particles whose noninformational degrees of freedom are nonfactorable. Phys Rev A 2013;87:042327.
[52] Pezzé L, Smerzi A. Phase sensitivity of a mach-zehnder interferometer. Phys Rev A 2006;73:011801(R).
[53] Svore KM, Freedman M. Faster phase estimation. Quan Inf Comput 2014;14:306.
[54] Ding X, He Y, Duan Z-C, et al. On-demand single photons with high extraction efficiency and near-Unity indistinguishability from a resonantly driven quantum dot in a micropillar. Phys Rev Lett 2016;116:020401.
[55] Somaschi N, Giesz V, De Santis L, et al. Near-optimal single-photon sources in the solid state. Nat Photonics 2016;10:340–5.
[56] Loredo JC, Zakaria NA, Somaschi N, et al. Scalable performance in solid-state single-photon sources. Optica 2016;3:433–40.
[57] Wang H, Duan Z-C, Li Y-H, et al. Near-transform-limited single photons from an efficient solid-state quantum emitter. Phys Rev Lett 2016;116:213601.
[58] Harris NC, Steinbrecher GR, Prabhu M, et al. Quantum transport simulations in a programmable nanophotonic processor. Nat Photonics 2017;11:447–52.

Niko Viggianiello obtained his Ph.D. degree in 2018 at Sapienza University of Rome, Italy, where he is working on quantum information and integrated photonics. His research activities focus on the validation of multi-photon quantum interference and, specifically, on the implementation of Boson Sampling experiments to achieve quantum computational advantage.

Fabio Sciarrino is professor and head of the Quantum Information Laboratory in the Department of Physics of Sapienza Università di Roma (www.quantumlab.it). He obtained his Ph.D. degree in 2004 with a thesis in experimental quantum optics. His researches include works on quantum metrology, fundamental tests of quantum mechanics, quantum teleportation and quantum communication. Recently he has contributed to the application of integrated photonics for quantum walks, Boson Sampling and optimal quantum machines.